

# Revealing Protein Structures in Solid-Phase Peptide Synthesis by $^{13}\text{C}$ Solid-State NMR: Evidence of Excessive Misfolding for Alzheimer's $\beta$

Songlin Wang<sup>†</sup> and Yoshitaka Ishii<sup>\*,†,‡</sup>

<sup>†</sup>Department of Chemistry, University of Illinois at Chicago, 845 West Taylor Street, Chicago, Illinois 60607, United States

<sup>‡</sup>Center for Structural Biology, University of Illinois at Chicago, 1100 South Ashland Street, Chicago, Illinois 60607, United States

**S** Supporting Information

**ABSTRACT:** Solid-phase peptide synthesis (SPPS) is a widely used technique in biology and chemistry. However, the synthesis yield in SPPS often drops drastically for longer amino acid sequences, presumably because of the occurrence of incomplete coupling reactions. The underlying cause for this problem is hypothesized to be a sequence-dependent propensity to form secondary structures through protein aggregation. However, few methods are available to study the site-specific structure of proteins or long peptides that are anchored to the solid support used in SPPS. This study presents a novel solid-state NMR (SSNMR) approach to examine protein structure in the course of SPPS. As a useful benchmark, we describe the site-specific SSNMR structural characterization of the 40-residue Alzheimer's  $\beta$ -amyloid ( $A\beta$ ) peptide during SPPS. Our 2D  $^{13}\text{C}/^{13}\text{C}$  correlation SSNMR data on  $A\beta(1-40)$  bound to a resin support demonstrated that  $A\beta$  underwent excessive misfolding into a highly ordered  $\beta$ -strand structure across the entire amino acid sequence during SPPS. This approach is likely to be applicable to a wide range of peptides/proteins bound to the solid support that are synthesized through SPPS.

Solid-phase peptide synthesis (SPPS) has been proven to be a highly effective technique for the production of proteins/peptides of an arbitrary amino acid sequence at high purity.<sup>1</sup> More recently, SPPS has been an indispensable tool for the construction of peptide/protein libraries for high-throughput screening in systems biology and drug development.<sup>2</sup> On the other hand, it is known that the coupling efficiency in SPPS is radically suppressed for long peptide sequences that exceed 30–50 residues.<sup>3</sup> Thus, chemical synthesis of a protein having a longer amino acid sequence often requires chemical ligation of shorter peptides,<sup>4</sup> which limits automation and high-throughput applications that are crucial in modern biology. The difficulties in the synthesis of longer peptides have been attributed to secondary structure formation through interchain aggregation and/or poor solvation of the growing peptide chains;<sup>3,5</sup> however, the detailed molecular mechanisms responsible for these observations are currently unknown. For example, a peptide in SPPS is elongated from the C-terminus to the N-terminus by repeated coupling of Fmoc- or Boc-protected amino acids; thus, a major hindrance due to the hypothesized misfolding in SPPS should arise from the structural transition or the lack of solvation at the N-terminal

regions. On the other hand, the N-terminal regions of proteins are often unstructured<sup>6</sup> and less likely to participate in the expected structure formation in SPPS. Therefore, site-specific structures of peptides/proteins in SPPS will provide valuable molecular-level insight into the controversies and challenges of synthesizing larger peptides/proteins.

Currently, very little is known about the structure of a protein or a long peptide (>20 residues) during SPPS, despite recent advances in structural biology. X-ray crystallography, a powerful method for protein structural determination, is not an option because of the noncrystalline nature of the heterogeneous solid support in SPPS. Characterization of peptides/proteins during SPPS by solution NMR or other spectroscopic methods has generally been limited because of the solid support (e.g., resin), which absorbs or scatters light and limits the resolution of solution NMR. A wide-line  $^2\text{D}$  solid-state NMR (SSNMR) study of resin-bound polyglycine [(gly- $d_2$ )<sub>*n*</sub>, *n* = 3–9] indicated a loss of mobility for the system when a critical length was exceeded (*n* > 5)<sup>7</sup> but did not provide any structural details or site specificity. High-resolution solution NMR<sup>8</sup> has been used to characterize resin-bound polyalanine<sup>9</sup> or saccharides.<sup>10</sup> However, the application of this method has been limited to only very short peptides (up to 10–15 residues) because of the restricted resolution for longer sequences. Thus, defining a detailed site-specific structure on a long peptide or protein in SPPS has been an intractable problem for nearly 50 years, since the introduction of SPPS by Merrifield.<sup>1</sup>

In this study, we propose high-resolution  $^{13}\text{C}$  SSNMR analysis of resin-bound proteins during SPPS in order to achieve the site-specific structural analysis for such systems. As an interesting benchmark, we selected the 40-residue  $\beta$ -amyloid ( $A\beta$ ) peptide because it is one of only a few biologically significant systems for which structures of both monomeric and misfolded forms have been reported. It is well-known that unstructured monomeric  $A\beta(1-40)$  self-assembles into  $\beta$ -sheet-rich amyloid fibrils, which are associated with Alzheimer's disease (AD).<sup>11</sup> Because of the great interest in  $A\beta$  for biomedical and biophysical studies,<sup>11,12</sup> including SSNMR studies,<sup>13,14</sup> the  $A\beta$  peptide has been a major target of SPPS.<sup>15</sup> Indeed, various SPPS methods have been proposed to overcome difficulties in SPPS.<sup>3,16</sup> However, there has been little experimental evidence regarding the structural features of  $A\beta$  in SPPS, which may provide critical insights into the mechanism

Received: July 27, 2011

Published: January 20, 2012

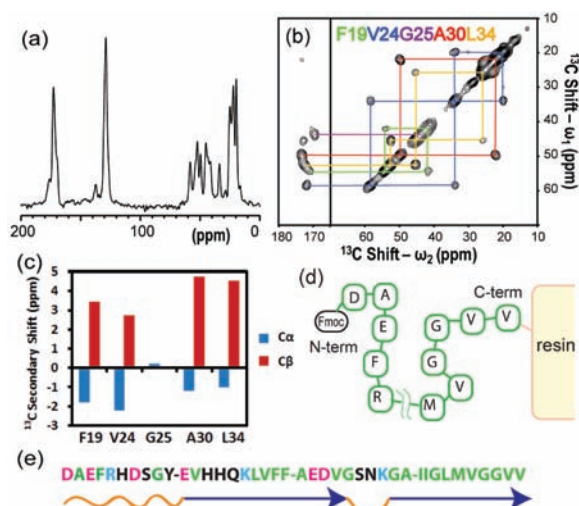


**Figure 1.** (a) 1D  $^{13}\text{C}$  CPMAS spectrum and (b) 2D  $^{13}\text{C}/^{13}\text{C}$  correlation SSMR spectrum of resin-bound  $A\beta(1-40)$  solvated with DCM shown with color-coded signal assignments (see the inset). The spinning speed was 20 kHz. The peptide was synthesized with uniformly  $^{13}\text{C}$ - and  $^{15}\text{N}$ -labeled amino acids at Phe-19, Val-24, Gly-25, Ala-30, and Leu-34. For synthesis of the sample, a standard Fmoc SPPS protocol was employed using NMP as a solvent and Fmoc-Val-Wang resin (0.22 mequiv/g) swollen with DCM. The resin was washed with DCM at the end of the synthesis. The data acquisition for (a) was started ca. 2 h after the synthesis. In (a) and (b), during the CP period, the  $^{13}\text{C}$  RF field amplitude was linearly swept from 46 to 63 kHz during a contact time of 1.0 ms, while the  $^1\text{H}$  RF amplitude was kept constant at 75 kHz. In (a), the experiment time was 17 min. The spectrum in (b) was obtained with an fpRFDR sequence.<sup>18</sup> During the mixing period, an fpRFDR  $^{13}\text{C}-^{13}\text{C}$  dipolar recoupling sequence with a mixing time of 1.6 ms and  $^{13}\text{C}$   $\pi$ -pulse widths of 15  $\mu\text{s}$  was used. The experiment time for (b) was 19 h. (c)  $^{13}\text{C}$  secondary chemical shift analysis of Phe-19, Val-24, Gly-25, Ala-30, and Leu-34 for  $A\beta(1-40)$  bound to  $A\beta$  resin. (d) Schematic representation of an  $A\beta$  peptide bound to resin. (e) Amino acid sequence of  $A\beta(1-40)$  peptide and the secondary structure of the amyloid fibril suggested by SSMR.<sup>19</sup> Blue arrows denote  $\beta$ -sheet regions, and orange loops denote unstructured or loop regions.

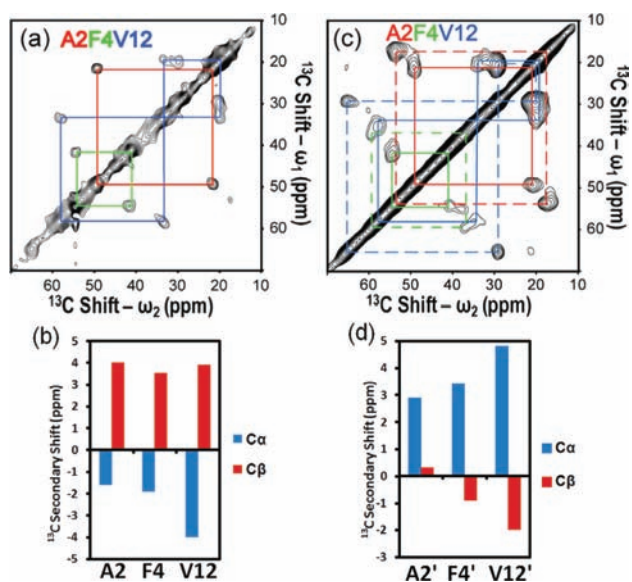
that prevents SPPS for  $A\beta$  and other long peptides. Here, with recent progress in biomolecular SSMR,<sup>17</sup> we revisit this long-standing problem. We report that  $^{13}\text{C}$  SSMR analysis using magic-angle spinning (MAS) serves as a probe that is very sensitive to site-specific structural properties of proteins in SPPS.

Figure 1a,b shows (a) 1D  $^{13}\text{C}$  cross-polarization MAS (CPMAS) and (b) 2D  $^{13}\text{C}/^{13}\text{C}$  correlation SSMR spectra of resin-bound  $A\beta(1-40)$  peptide labeled at several sites between residues 19 and 34 with uniformly  $^{13}\text{C}$ - and  $^{15}\text{N}$ -labeled amino acids (see the caption). The sample was prepared by standard Fmoc-based SPPS using Wang resin as a solid support [see below and the Supporting Information (SI) for details] and packed in a rotor after washing with dichloromethane (DCM). As mentioned above, the C-terminus of a peptide is bound to the resin in Fmoc-based SPPS, and Fmoc-protected amino acids are repeatedly coupled to the N-terminus (Figure 1d). Thus, these labeled sites reflect peptide conformations closer to the resin support. In monomeric form,  $A\beta(1-40)$  is known to exhibit largely a random-coil structure with a high degree of dynamics.<sup>20</sup> Initially, we expected considerable dynamics and structural heterogeneity of the resin-bound peptide solvated with DCM, which would result in weaker and broader  $^{13}\text{C}$

signals in the  $^{13}\text{C}$  CPMAS spectra. Unexpectedly, however, strong signal intensities were observed in the 1D  $^{13}\text{C}$  CPMAS spectrum (Figure 1a); this confirmed the lack of motions in the area, because large-amplitude motions would have averaged out dipolar couplings and suppressed  $^{13}\text{C}$  signals through CP. More surprisingly, the cross-peaks for the 2D  $^{13}\text{C}/^{13}\text{C}$  SSMR spectrum (Figure 1b) showed reasonably narrow line widths (1.9–2.8 ppm) considering that the system embedded in resin was noncrystalline and that the line widths include Gaussian broadening (ca. 1 ppm) and broadening due to  $^{13}\text{C}-^{13}\text{C}$   $J$  couplings. The line widths were comparable to those of  $A\beta(1-40)$  amyloid fibrils, which are known to have a high degree of structural order.<sup>19,21</sup> Because chemical shifts are sensitive to the conformation of a peptide, this finding clearly suggests the formation of a highly ordered conformation, which has not been predicted in previous studies for this system bound to a heterogeneous resin matrix.

Using the well-resolved resonances and signal assignments shown in Figure 1b, we analyzed secondary structures of resin-bound  $A\beta(1-40)$  using secondary  $^{13}\text{C}$  shifts ( $\Delta$ ) for the  $^{13}\text{C}_{\alpha}$  (blue) and  $^{13}\text{C}_{\beta}$  (red) shifts, which represent the deviation of the experimental shift ( $\delta_{\text{exp}}$ ) from the corresponding shift for random-coil model peptides ( $\delta_{\text{rc}}$ )<sup>22</sup> (i.e.,  $\Delta = \delta_{\text{exp}} - \delta_{\text{rc}}$ ; see Table S1 in the SI). The negative and positive  $\Delta$  values for  $^{13}\text{C}_{\alpha}$  and  $^{13}\text{C}_{\beta}$ , respectively, suggest the formation of extended  $\beta$ -strand structures over the hydrophobic core region in  $A\beta(1-40)$ .<sup>22</sup> It is noteworthy that in Figure 1b, only a single cross-peak was observed for a chemically bonded  $^{13}\text{C}-^{13}\text{C}$  pair, unlike some amyloid fibrils, which often show multiple cross-peaks for a  $^{13}\text{C}-^{13}\text{C}$  pair due to structural polymorphs. This result suggests a remarkable finding that the  $A\beta(1-40)$  peptide not only aggregates in the course of SPPS but also misfolds into a single, well-defined  $\beta$ -strand conformer. For the SPPS of  $A\beta$ , we used low-loading resin (0.22 mequiv/g in a dry state), yet the estimated concentration of  $A\beta$  in resin swollen with a solvent is in on the order of 40 mM, which is typically more than sufficient to introduce misfolding of  $A\beta(1-40)$  in an aqueous solution. On the other hand, because of the solid support, peptides from SPPS have very limited translational diffusion, unlike a peptide in a solution. Thus, it was not trivial to predict misfolding and a high degree of structural order for  $A\beta$  in SPPS. The features of this SSMR spectrum, which was collected ca. 2 h after the synthesis, were unaltered over several days (see Figure S4 in the SI). This result suggests that the peptides were misfolded and that their conformation reached the equilibrium state in the solvent reasonably quickly. We confirmed that with the exception of mild line broadening, the chemical shifts for this sample were unchanged by the removal of DCM (Figure S4c). We also collected a 1D  $^{13}\text{C}$  CPMAS spectrum of the same resin-bound  $A\beta$  peptide sample solvated with *N*-methyl-2-pyrrolidone (NMP), which was obtained without a DCM wash, although the flammable nature of NMP prevented us from testing a time-consuming 2D experiment. The 1D spectrum for this sample with NMP was found to be very similar to that shown in Figure 1a. Thus, the solvent effects on  $^{13}\text{C}$  shifts are negligible. Notably, the  $\beta$ -strand structures likely are stable without the solvents.

We next examined the site-specific structure of the N-terminal residues of  $A\beta(1-40)$  in SPPS. In previous studies of amyloid fibrils, it was reported that the first 10 residues of  $A\beta(1-40)$  in the N-terminus are disordered or mobile.<sup>19</sup> On the other hand, we found that it was difficult to couple efficiently the last 3–4 amino acids of the N-terminus of  $A\beta(1-$



**Figure 2.** (a) Aliphatic region of a 2D  $^{13}\text{C}/^{13}\text{C}$  chemical-shift correlation SSNMR spectrum of resin-bound  $\text{A}\beta(1-40)$  solvated with DCM, with color-coded signal assignments (red, Ala-2; green, Phe-4; blue, Val-12). The peptide was labeled with uniformly  $^{13}\text{C}$ - and  $^{15}\text{N}$ -labeled amino acids at Ala-2, Phe-4, and Val-12. The sample preparation and SSNMR method are the same as those in Figure 1b except for the labeled positions. The experiment time was 31 h. (b)  $^{13}\text{C}$  secondary chemical shift analysis of Ala-2, Phe-4, and Val-12 for  $\text{A}\beta(1-40)$  bound to  $\text{A}\beta$  resin. (c) Aliphatic region of a 2D  $^{13}\text{C}/^{13}\text{C}$  correlation SSNMR spectrum for the same resin-bound  $\text{A}\beta(1-40)$  sample after the removal of DCM, with color-coded assignments. Dashed lines show the new resonances that appeared after removal of DCM. The experiment time was 31 h. (d)  $^{13}\text{C}$  secondary chemical shift analysis of the new resonances of Ala-2, Phe-4, and Val-12 for the dried resin-bound  $\text{A}\beta(1-40)$  sample used in (c).

40) in SPPS without multiple couplings. Therefore, we decided to examine whether misfolding of  $\text{A}\beta$  in SPPS involves three residues (Ala-2, Phe-4, Val-12) in the N-terminal region using 2D  $^{13}\text{C}/^{13}\text{C}$  correlation SSNMR for  $\text{A}\beta(1-40)$  in which uniformly  $^{13}\text{C}$ - and  $^{15}\text{N}$ -labeled amino acids were introduced at these sites (Figure 2a). Although the normalized signal intensities were weaker than those observed in Figure 1b, sharp resonances were observed for the cross-peaks for all of these residues. Surprisingly, analysis of the secondary chemical shifts showed that  $^{13}\text{C}_\alpha$  and  $^{13}\text{C}_\beta$  exhibited negative and positive shifts, respectively (Figure 2b), suggesting the formation of a  $\beta$ -strand in the N-terminal region up to Ala-2. Quantitative analysis using TALOS software also confirmed the  $\beta$ -strand formation (Table S1). This finding confirms the excessive misfolding of the N-terminal residues of  $\text{A}\beta(1-40)$  in SPPS, which has not been previously observed, even for the  $\text{A}\beta(1-40)$  fibril. This is the first example demonstrating excessive misfolding of the  $\beta$ -strand in the N-terminal region for a relatively long peptide in SPPS.

These new data indicate that some dynamics is involved in the N-terminal region of resin-bound  $\text{A}\beta$ . We first noticed that the signal-to-noise ratio in Figure 2a was less than that in observed in Figure 1b for the unit sample and unit number of scans. The integrated signal intensity of the aliphatic region (10–70 ppm) in the 1D spectrum normalized by sample amount and the numbers of  $^{13}\text{C}$  species and scans was less than what was observed in Figure 1a (ca. 67%). To examine the effects of the solvent and dynamics, we obtained a 2D  $^{13}\text{C}/^{13}\text{C}$

spectrum for  $\text{A}\beta(1-40)$  for the same sample after removing the solvent (Figure 2c). Interestingly, new resonances emerged for Ala-2, Phe-4, and Val-12 in the spectrum of the sample without the solvent (dashed lines in Figure 2c). The new resonances for Phe-4, which did not have very clear separation from the peaks for Val-12 in Figure 2c, were confirmed by a dipolar-assisted rotational resonance (DARR) experiment (see Figure S6). Remarkably, the secondary chemical shifts for these new resonances (Figure 2d) indicate  $\alpha$ -helical structure for Ala-2, Phe-4, and Val-12 (Table S1) on the basis of an analysis using TALOS software.<sup>23</sup> The integral intensities of these peaks were comparable to those for the resonances corresponding to the  $\beta$ -strand structure (ca. 120% for Ala-2 with respect to the corresponding peak for the  $\beta$ -strand species). The slightly broader line widths observed in Figure 2c may be attributed to the fact that the conformational heterogeneity becomes fixed after solvent removal. The present SSNMR results suggest for the first time that unlike amyloid fibrils of  $\text{A}\beta$ , approximately half of the population of  $\text{A}\beta(1-40)$  exhibits excessive misfolding into a rigid  $\beta$ -strand within the N-terminal region during SPPS, while the rest of the population possesses a helical structure. Because the latter conformer is not visible in the 2D spectrum with solvent (Figure 2a), it is likely that the highly dynamic nature of the non- $\beta$  conformer suppresses the CP in the presence of solvent (also see Figure S5). Our preliminary data using  $^{13}\text{C}$ - $^1\text{H}$  rotational-echo double-resonance (REDOR) experiments for  $^{13}\text{C}_\alpha$  of Ala-2 and Ala-30 for  $\text{A}\beta$  in DCM (see the SI) showed that these residues in the  $\beta$ -strand structures have order parameters close to 1 ( $S = 0.84-0.86$ ; Table S2), suggesting a lack of motion. These data clearly demonstrate that the proposed novel SSNMR analysis allows us to determine the site-specific structural and dynamical information, including the presence of the two conformations in the N-terminus of  $\text{A}\beta$  during SPPS. It is quite possible that the excessive misfolding into an extended  $\beta$ -strand structure at the N-terminus prevents coupling of additional amino acids. In SPPS, the efficiency of coupling ( $f$ ) for each amino acid usually needs to be extremely high ( $f > 99\%$ ), as the yield ( $\xi$ ) is approximately given by  $\xi = f^N$ , where  $N$  denotes the number of amino acid residues. Assuming that  $f$  is ca. 50% (or 0.5), the yield is suppressed down to  $\xi = 0.8-3\%$  even for a short sequence having 5–7 residues. The population of the misfolded species obtained by SSNMR (ca. 50%) implies that a drastic decline in the synthesis efficiency of SPPS could be explained by the excessive misfolding across the sequence.

In conclusion, we have presented an approach for obtaining site-specific analyses of protein structures during SPPS. Despite the long history of SPPS and its effectiveness in biological applications, no site-specific structures have been reported for proteins bound to a solid support in SPPS. We have demonstrated that our SSNMR approach is highly effective in elucidating structural and dynamical features of long peptides or proteins during SPPS using  $\text{A}\beta(1-40)$  as a notable benchmark system of a long hydrophobic peptide. This is the first example to report that a site-specific structure can be defined for aggregated proteins during SPPS. Since a relatively small quantity of isotope-labeled peptide-bound resin (5–10 mg) is required for multidimensional  $^{13}\text{C}$  SSNMR analysis, our approach opens an avenue toward the routine analysis of protein structures during SPPS. Moreover, our SSNMR data of  $\text{A}\beta(1-40)$  peptide bound to a heterogeneous resin have demonstrated that the resin-bound peptide undergoes misfolding into a unique conformation having a highly ordered  $\beta$ -

strand structure during the course of SPPS. To our surprise, the  $\beta$ -strand region of A $\beta$ (1–40) bound to resin spans the entire sequence, including the N-terminal region, which is unstructured and dynamic for A $\beta$ (1–40) even in amyloid fibrils. The observation of excessive misfolding provides excellent insight into how the structural evolution of A $\beta$  can interfere with efficient coupling in the N-terminus of a peptide during SPPS. These findings clearly indicate major structural problems in efficient synthesis of A $\beta$  and possibly other proteins by SPPS. Although additional studies are needed to identify whether such excessive misfolding into highly rigid  $\beta$ -strand structures is commonly observed during SPPS of other peptides/proteins, the SSNMR approach presented here is likely applicable to a broad range of proteins and may provide a critical structural foundation for designing more efficient SPPS schemes. For analysis of long peptides with redundant amino acids, the present method using 2D  $^{13}\text{C}/^{13}\text{C}$  correlation requires a considerable number of labeled samples to examine the entire sequence, as commonly observed for SSNMR analysis of heterogeneous peptides. For such systems, sequential assignments may offer more efficient structural analysis in future studies.

**Materials and Methods.**  $^{13}\text{C}$ - and  $^{15}\text{N}$ -labeled A $\beta$ (1–40) was synthesized with standard Fmoc-based synthesis as previously described<sup>14</sup> using an ABI 433 peptide synthesizer and the Fmoc-Val-Wang resin. After synthesis, the Fmoc group was removed and the resin was washed with DCM. All of the SSNMR experiments were conducted at a static field of 9.4 T using a Varian InfinityPlus 400 NMR spectrometer and a home-built 2.5 mm MAS triple-resonance probe. Other details are described in the SI.

## ■ ASSOCIATED CONTENT

### ● Supporting Information

Detailed experimental procedures for SSNMR and SPPS, additional SSNMR data, and complete refs 2a and 12b. This material is available free of charge via the Internet at <http://pubs.acs.org>.

## ■ AUTHOR INFORMATION

### Corresponding Author

yishii@uic.edu

## ■ ACKNOWLEDGMENTS

The development of the novel SSNMR approach was primarily supported by the NSF (CHE 957793). Our synthesis efforts of A $\beta$  in this study were in part supported by the Dreyfus Foundation Teacher-Scholar Award Program and the NIH (GM098033). We are grateful to Mr. S. Parthasarathy for providing a peptide sample for our initial studies.

## ■ REFERENCES

- (1) Merrifield, R. B. *J. Am. Chem. Soc.* **1963**, *85*, 2149. Merrifield, B. *Science* **1986**, *232*, 341.
- (2) (a) Beyer, M.; et al. *Science* **2007**, *318*, 1888. (b) Chen, X. Y.; Gambhir, S. S. *Nat. Chem. Biol.* **2006**, *2*, 351. (c) Peng, L.; Liu, R. W.; Marik, J.; Wang, X. B.; Takada, Y.; Lam, K. S. *Nat. Chem. Biol.* **2006**, *2*, 381. (d) Breitling, F.; Nesterov, A.; Stadler, V.; Felgenhauer, T.; Bischoff, F. R. *Mol. BioSyst.* **2009**, *5*, 224.
- (3) Kent, S. B. H. *Annu. Rev. Biochem.* **1988**, *57*, 957. Coin, I.; Beyermann, M.; Bienert, M. *Nat. Protoc.* **2007**, *2*, 3247.
- (4) Dawson, P. E.; Muir, T. W.; Clark-Lewis, I.; Kent, S. B. H. *Science* **1994**, *266*, 776.
- (5) Larsen, B. D.; Christensen, D. H.; Holm, A.; Zillmer, R.; Nielsen, O. F. *J. Am. Chem. Soc.* **1993**, *115*, 6247.
- (6) Lobanov, M. Y.; Furlatova, E. I.; Bogatyreva, N. S.; Roytberg, M. A.; Galzitskaya, O. V. *PLoS Comput. Biol.* **2010**, *6*, No. e1000958.
- (7) Ludwick, A. G.; Jelinski, L. W.; Live, D.; Kintanar, A.; Dumais, J. *J. Am. Chem. Soc.* **1986**, *108*, 6493.
- (8) Keifer, P. A.; Baltusis, L.; Rice, D. M.; Tymiak, A. A.; Shoolery, J. N. *J. Magn. Reson., Ser. A* **1996**, *119*, 65. Sarkar, S. K.; Garigipati, R. S.; Adams, J. L.; Keifer, P. A. *J. Am. Chem. Soc.* **1996**, *118*, 2305. Fitch, W. L.; Detre, G.; Holmes, C. P.; Shoolery, J. N.; Keifer, P. A. *J. Org. Chem.* **1994**, *59*, 7955.
- (9) Warrass, R.; Wieruszkeski, J. M.; Boutillon, C.; Lippens, G. *J. Am. Chem. Soc.* **2000**, *122*, 1789.
- (10) Loening, N. M.; Kanemitsu, T.; Seeberger, P. H.; Griffin, R. G. *Magn. Reson. Chem.* **2004**, *42*, 453.
- (11) Selkoe, D. J. *Nat. Cell Biol.* **2004**, *6*, 1054.
- (12) (a) Klein, W. L.; Stine, W. B.; Teplow, D. B. *Neurobiol. Aging* **2004**, *25*, 569. (b) Noguchi, A.; et al. *J. Biol. Chem.* **2009**, *284*, 32895.
- (13) Petkova, A. T.; Leapman, R. D.; Guo, Z. H.; Yau, W. M.; Mattson, M. P.; Tycko, R. *Science* **2005**, *307*, 262. Parthasarathy, S.; Long, F.; Miller, Y.; Xiao, Y.; Thurber, K.; McElheny, D.; Ma, B.; Nussinov, R.; Ishii, Y. *J. Am. Chem. Soc.* **2011**, *133*, 3390. Ahmed, M.; Davis, J.; Aucoin, D.; Sato, T.; Ahuja, S.; Aimoto, S.; Elliott, J. I.; Van Nostrand, W. E.; Smith, S. O. *Nat. Struct. Mol. Biol.* **2010**, *17*, 561. de Planque, M. R. R.; Raussens, V.; Contera, S. A.; Rijkers, D. T. S.; Liskamp, R. M. J.; Ruysschaert, J. M.; Ryan, J. F.; Separovic, F.; Watts, A. *J. Mol. Biol.* **2007**, *368*, 982.
- (14) Chimon, S.; Ishii, Y. *J. Am. Chem. Soc.* **2005**, *127*, 13472. Chimon, S.; Shaibat, M. A.; Jones, C. R.; Calero, D. C.; Aizezi, B.; Ishii, Y. *Nat. Struct. Mol. Biol.* **2007**, *14*, 1157.
- (15) Tickler, A. K.; Barrow, C. J.; Wade, J. D. *J. Pept. Sci.* **2001**, *7*, 488. Sohma, Y.; Kiso, Y. *ChemBioChem* **2006**, *7*, 1549. Zarandi, M.; Soos, K.; Fulop, L.; Bozso, Z.; Datki, Z.; Toth, G. K.; Penke, B. *J. Pept. Sci.* **2007**, *13*, 94.
- (16) Canne, L. E.; Botti, P.; Simon, R. J.; Chen, Y.; Dennis, E. A.; Kent, S. B. H. *J. Am. Chem. Soc.* **1999**, *121*, 8720. Dawson, P. E.; Kent, S. B. H. *Annu. Rev. Biochem.* **2000**, *69*, 923.
- (17) Baldus, M. *Curr. Opin. Struct. Biol.* **2006**, *16*, 618. McDermott, A. E. *Annu. Rev. Biophys.* **2009**, *38*, 385. Jaroniec, C. P.; MacPhee, C. E.; Astrof, N. S.; Dobson, C. M.; Griffin, R. G. *Proc. Natl. Acad. Sci. U.S.A.* **2002**, *99*, 16748. Castellani, F.; van Rossum, B.; Diehl, A.; Schubert, M.; Rehbein, K.; Oschkinat, H. *Nature* **2002**, *420*, 98. Lange, A.; Giller, K.; Hornig, S.; Martin-Eauclaire, M. F.; Pongs, O.; Becker, S.; Baldus, M. *Nature* **2006**, *440*, 959. Pintacuda, G.; Giraud, N.; Picrattelli, R.; Bockmann, A.; Bertini, I.; Emsley, L. *Angew. Chem., Int. Ed.* **2007**, *46*, 1079. Curtis-Fisk, J.; Spencer, R. M.; Weliky, D. P. *J. Am. Chem. Soc.* **2008**, *130*, 12568. Helmus, J. J.; Surewicz, K.; Nadaud, P. S.; Surewicz, W. K.; Jaroniec, C. P. *Proc. Natl. Acad. Sci. U.S.A.* **2008**, *105*, 6284. Wasmer, C.; Lange, A.; Van Melckebeke, H.; Siemer, A. B.; Riek, R.; Meier, B. H. *Science* **2008**, *319*, 1523. Cady, S. D.; Schmidt-Rohr, K.; Wang, J.; Soto, C. S.; DeGrado, W. F.; Hong, M. *Nature* **2010**, *463*, 689. Bertini, I.; Luchinat, C.; Parigi, G.; Ravera, E.; Reif, B.; Turano, P. *Proc. Natl. Acad. Sci. U.S.A.* **2011**, *108*, 10396.
- (18) Ishii, Y. *J. Chem. Phys.* **2001**, *114*, 8473.
- (19) Petkova, A. T.; Ishii, Y.; Balbach, J. J.; Antzutkin, O. N.; Leapman, R. D.; Delaglio, F.; Tycko, R. *Proc. Natl. Acad. Sci. U.S.A.* **2002**, *99*, 16742.
- (20) Riek, R.; Guntert, P.; Dobeli, H.; Wipf, B.; Wuthrich, K. *Eur. J. Biochem.* **2001**, *268*, 5930.
- (21) Tycko, R. Q. *Rev. Biophys.* **2006**, *39*, 1.
- (22) Spera, S.; Bax, A. *J. Am. Chem. Soc.* **1991**, *113*, 5490.
- (23) Cornilescu, G.; Delaglio, F.; Bax, A. *J. Biomol. NMR* **1999**, *13*, 289.